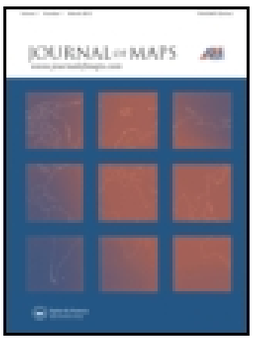

Journal of Maps

ISSN: (Print) 1744-5647 (Online) Journal homepage: http://www.tandfonline.com/loi/tjom20

Structural analysis of a subduction-related contact in southern Sesia-Lanzo Zone (Austroalpine Domain, Italian Western Alps)

Michela Cantù, Luca Spaggiari, Michele Zucali, Davide Zanoni & M. Iole Spalla

To cite this article: Michela Cantù, Luca Spaggiari, Michele Zucali, Davide Zanoni & M. Iole Spalla (2016): Structural analysis of a subduction-related contact in southern Sesia-Lanzo Zone (Austroalpine Domain, Italian Western Alps), Journal of Maps, DOI: 10.1080/17445647.2016.1155925

To link to this article: http://dx.doi.org/10.1080/17445647.2016.1155925

JOURNAL OF MAPS, 2016
http://dx.doi.org/10.1080/17445647.2016.1155925

Taylor & Francis
Taylor & Francis Group

SCIENCE

Structural analysis of a subduction-related contact in southern Sesia-Lanzo Zone (Austroalpine Domain, Italian Western Alps)

Michela Cantù[a], Luca Spaggiari[b], Michele Zucali[b], Davide Zanoni[b] and M. Iole Spalla[b]

[a]Dipartimento di Scienze della Terra e dell'Ambiente, Università degli Studi di Pavia, Pavia, Italy; [b]Dipartimento di Scienze della Terra "A. Desio", Università degli Studi di Milano, Milano, Italy

ABSTRACT

A new foliation trajectory map at 1:10000 scale, represented here with an interpretative structural map, is derived from an original field analysis at 1:5000 scale in the southern Sesia-Lanzo Zone (SLZ). It shows the relative chronology of overprinting foliations, characterised by the mineral assemblages that mark superposed fabrics in each rock type. This map and the associated cross-sections, which synthesise the 3D structural outline of the tectonic contact between the Eclogitic Micaschists Complex (EMC), the Rocca Canavese Thrust Sheets and the Lanzo Ultramafic Complex, allow the correlation of the structural and metamorphic imprints that developed in these crustal and mantle complexes during Alpine subduction. Furthermore, the map and cross-sections allow the immediate perception of the metamorphic environments in which the structural imprints developed in each complex successively under eclogite, blueschist and greenschist facies conditions. The represented structural and metamorphic evolution of the southern end of the SLZ (internal Western Alps) has been inferred based on multiscale structural analysis. The dominant fabrics at the regional scale are two superposed mylonitic foliations that developed under blueschist and greenschist facies conditions, respectively. Metamorphic assemblages underlying the successive fabrics in the different metamorphic complexes allow us to identify contrasting metamorphic evolutions indicating that the tectonic contacts between the EMC, the Rocca Canavese Thrust Sheets and the Lanzo Ultramafic Complex developed under blueschist facies conditions and were successively reactivated during the greenschist facies retrogression.

ARTICLE HISTORY
Received 13 July 2015
Revised 20 December 2015
Accepted 11 February 2016

KEYWORDS
Foliation trajectory maps; multi-scale structural analysis; blueschist/eclogite facies rocks; Eclogitic Micaschists Complex; Rocca Canavese Thrust Sheets; Lanzo Massif

1. Introduction

The Sesia-Lanzo Zone (SLZ; Figure 1) is the widest portion of continental crust re-equilibrated under eclogite-facies conditions during early Alpine (Late Cretaceous) subduction in the Western Alps (e.g. Handy & Oberhaensli, 2004; Hunziker, Desmons, & Hurford, 1992; Regis et al., 2014; Roda, Spalla, & Marotta, 2012; Rubatto et al., 2011). The peculiar metamorphic evolution of the SLZ, characterised by a high P/T ratio, drives the interpretation that its exhumation was accomplished before the onset of continental collision, when oceanic lithosphere was still subducting (e.g. Avigad, 1996; Roda, Marotta, & Spalla, 2010; Spalla, Lardeaux, Dal Piaz, Gosso, & Messiga, 1996; Zucali & Spalla, 2011; Zucali, Spalla, & Gosso, 2002). Three main lithologic complexes have been traditionally recognised in the SLZ (e.g. Compagnoni et al., 1977; Dal Piaz, Hunziker, & Martinotti, 1972): (i) the Gneiss Minuti complex (GMC), (ii) the Eclogitic Micaschists complex (EMC) and (iii) the II Dioritic-Kinzigitic Zone (IIDK). The IIDK consists of kilometric lenses of acidic and mafic granulites that do not record the eclogitic re-equilibration. The EMC and GMC, both pervasively eclogitised, mainly differ in the volume percentage of greenschist re-equilibration (Spalla, Lardeaux, Dal Piaz, & Gosso, 1991; Stuenitz, 1989). Another metamorphic complex has been subsequently described along the internal boundary of the southern SLZ, and named the Rocca Canavese Thrust Sheets (RCT; Pognante, 1989a). The RCT has been distinguished by its significantly different tectono-thermal Alpine evolution (Figure 1), in which the recorded peak P occurred under very low-temperature conditions and at lower pressures compared to EMC and GMC rocks (Pognante, 1989a, 1989b). The detailed petrologic analysis of this complex was subsequently integrated by structural analysis to unravel the grid of superposed synmetamorphic foliations in the two adjacent crustal complexes (EMC and RCT) that form the internal part of the southern SLZ (Spalla & Zulbati, 2003). The goal of this new map is to integrate the previous work and extend the structural analysis to the mantle rocks of the Lanzo Massif (LM) to infer the earlier detectable structural and metamorphic imprints that affect these crustal and mantle complexes deeply involved in the Alpine subduction system after their exhumation at shallow depth during Permian-Triassic times (Lardeaux & Spalla, 1991; Pelletier & Muentener, 2006; Pognante, 1991; Pognante, Talarico, & Benna, 1987; Rebay & Spalla, 2001; Roda et al., 2012; Spalla, De Maria, Gosso, Miletto, & Pognante, 1983; Wogelius & Finley, 1989).

CONTACT Michele Zucali michele.zucali@unimi.it

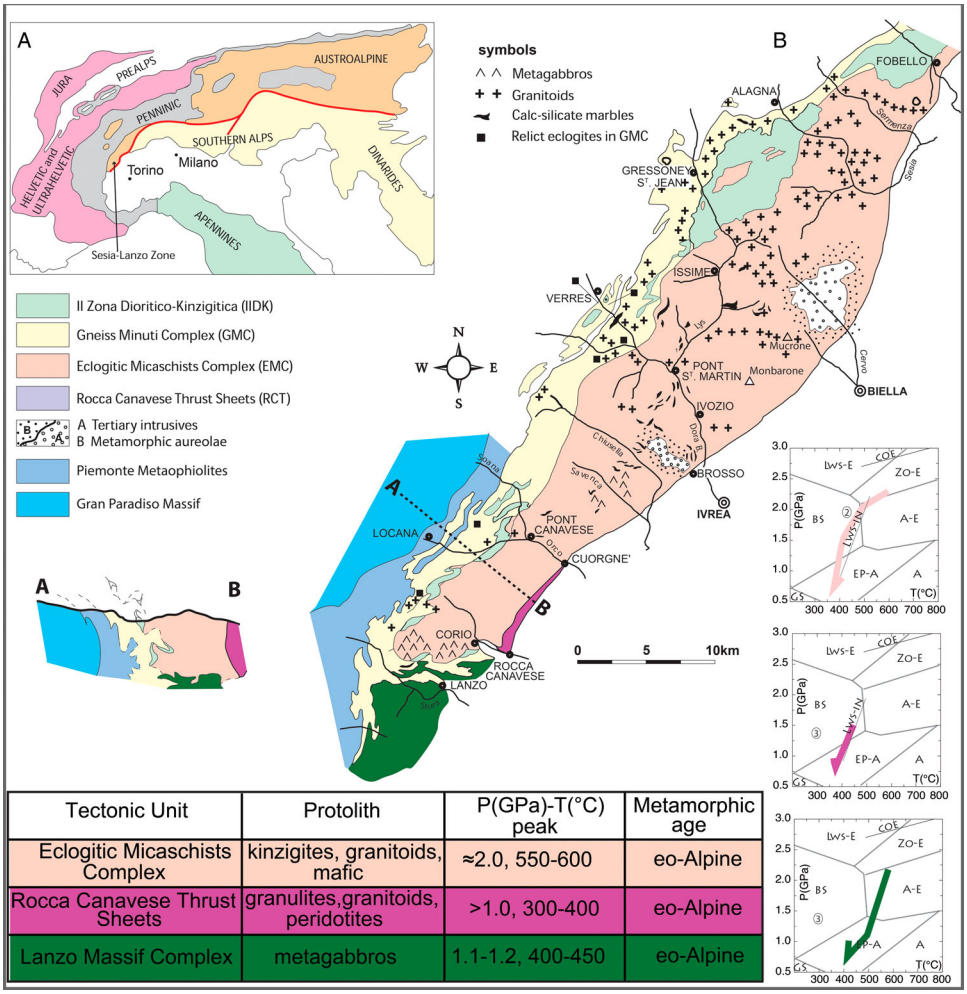

Tectonic Unit	Protolith	P(GPa)-T(°C) peak	Metamorphic age
Eclogitic Micaschists Complex	kinzigites, granitoids, mafic	≈2.0, 550-600	eo-Alpine
Rocca Canavese Thrust Sheets	granulites,granitoids, peridotites	>1.0, 300-400	eo-Alpine
Lanzo Massif Complex	metagabbros	1.1-1.2, 400-450	eo-Alpine

Figure 1. (a) Tectonic outline of the Alps. (b) Simplified geological map of the Sesia-Lanzo Zone modified after Zucali and Spalla (2011). P–T paths represent the Alpine metamorphic evolution of the EMC and RCT in the southern portion of the SLZ, redrawn after Pognante (1989a, 1989b), and the northern Lanzo Massif (ML), redrawn by Pelletier and Muentener (2006). The cross-section A-B is modified after Pognante et al. (1989a). The table shows protoliths, physical conditions of Alpine metamorphism and suggested metamorphic ages for each unit.

An additional goal is the reconstruction of the structural outline of the tectonic contacts between the three metamorphic complexes. For this purpose, a detailed foliation trajectory map has been synthesised from original fieldwork at 1:5000 scale and has been integrated with the interpretative map. The relative chronology of superposed foliations is shown on the map by the foliation trajectory symbols that represent the interpolation of seams of the foliation orientation data. The metamorphic environment in which successive fabrics developed, as inferred by mineral assemblages marking successive foliations in each rock type, is indicated by different colours. In this way, details of the relative chronology of structural imprints and metamorphic environments are independently shown and precisely located in space.

2. Geological outline

The particularly high P/T ratio characterising the Alpine evolution of this portion of the Austroalpine continental crust facilitated the preservation of pre-Alpine relic assemblages from granulite to greenschist facies conditions in marbles, metapelites, metagranitoids, metagabbros, amphibolites, and mafic and acidic granulites in Alpine low-strain domains (Compagnoni et al., 1977; Dal Piaz, Gosso, & Martinotti, 1971; Dal Piaz et al., 1972; Gosso, 1977; Lardeaux, 1981; Lardeaux & Spalla, 1991; Rebay & Spalla, 2001; Spalla et al., 1983; Williams & Compagnoni, 1983; Zucali, 2011 and references therein). The granulite to amphibolite pre-Alpine PT evolution has been interpreted as representative of an extension-related uplift, representing the first part of the exhumation path of the Adriatic lower continental crust up to very shallow crustal level, during Permian-Triassic times (e.g. Lardeaux & Spalla, 1991; Rebay & Spalla, 2001), as envisaged in other portions of the Austroalpine and Southalpine continental crust (e.g. Bertotti, Siletto, & Spalla, 1993; Bertotti & der Voorde, 1994; Dal Piaz, 1993; Diella, Spalla, & Tunesi, 1992; Handy, Franz, Heller, Janott, & Zurbriggen, 1999; Manzotti & Zucali, 2013; Marotta, Spalla, & Gosso, 2009; Schuster, Scharbert, Abart, & Frank, 2001; Schuster & Stuewe, 2008; Spalla et al., 2014). Early Alpine

high pressure–low temperature metamorphism of the SLZ (e.g. Cenki-Tok et al., 2011; Handy & Oberhaensli, 2004; Hunziker, 1974; Hunziker et al., 1992; Oberhaensli, Hunziker, Martinotti, & Stern, 1985; Regis et al., 2014; Rubatto, 1998; Rubatto, Gebauer, & Compagnoni, 1999; Rubatto et al., 2011; Stoeckhert, Jaeger, & Voll, 1986; Zucali & Spalla, 2011) is variably recorded across the four different metamorphic complexes (Roda et al., 2012 and references therein), which are schematically represented in Figure 1. The IIDK consists of km-sized lenses of lower continental crust that escaped the Alpine eclogitic re-equilibration, whereas the EMC and the GMC are pervasively eclogitised and variably record the uplift-related greenschist re-equilibration. The GMC is widely greenschist re-equilibrated and marks the continent-ocean tectonic boundary, which was active during the subduction and exhumation of the SLZ and meta-ophiolites. The greenschist re-equilibration is generally associated with widespread mylonitic textures (Babist, Handy, Konrad-Scmolke, & Hammerschmidt, 2006; Spalla et al., 1983, 1991; Stuenitz, 1989; Wheeler & Butler, 1993). The EMC constitutes the innermost part of the SLZ, where the exhumation-related greenschist imprint is confined to discrete shear zones (e.g. Babist et al., 2006; Zucali et al., 2002) and is more pervasive towards the inner boundary with the Southern Alps, marked by the Periadriatic Lineament. The RCT consists of thin crustal slices located along the eastern margin of the southern SLZ and extending from Rocca Canavese to Courgnè, as shown on the map and in Figure 1 (Pognante, 1989a, 1989b). This complex consists of pre-Alpine granulites, serpentinised tectonitic lherzolites, glaucophane-bearing schists and metagranitoids. The thin tectonic slices of the RCT are separated by Alpine blueschist mylonitic horizons, and their metamorphic evolution is considerably different from that of the other SLZ complexes (e.g. Pognante, 1989a; Spalla & Zulbati, 2003). In serpentinites small pods, generally metric, still preserve clino- and orthopyroxene (Barnes et al., 2014; Spalla & Zulbati, 2003). According to the literature, the eclogite-facies conditions affecting the EMC and the GMC are not recorded in the RCT (Pognante, 1989a), and after the blueschist facies re-equilibration, RCT rocks experienced a low-pressure vs. low- to very low-temperature re-equilibration. Based exclusively on the inferred metamorphic evolutions, the coupling between the EMC, GMC and RCT has been interpreted to have occurred in blueschist facies conditions, synchronous with the early exhumation stages of the EMC (Pognante, 1989b).

The LM comprises plagioclase and spinel lherzolite, pyroxenite and dunite surrounded and partially cut by serpentinite (e.g. Boudier, 1978; Nicolas, 1974; Piccardo, 2010; Piccardo, Zanetti, Pruzzo, & Padovano, 2007). The Alpine high-pressure metamorphism of LM rocks is heterogeneously recorded in metagabbros, peridotites and associated metasediments (Kienast & Pognante, 1988; Pelletier & Muentener, 2006). According to structural analysis, the western part of the southern boundary between the SLZ and the LM has been deformed since the early stages of Alpine deformation history and developed under HP conditions (Spalla et al., 1983).

3. Mapping techniques

The structural map presented here (Main Map) synthesises information on the successive fabric elements and the related mineral assemblages in the polydeformed rocks constituting crustal and mantle units, piled up in a subduction complex. The rocks are described and mapped based on their mineral compositions. Mapped structural elements consist of lithologic boundaries, axial plane foliations and lineations or axial plane trajectories, distinguished using overprinting relationships and the mineralogical support of these fabrics. Foliation trajectories are represented as coloured traces that are associated with standard lithological information: different colours and number of dots represent the metamorphic facies and relative chronology of the development of subsequent foliations, respectively.

Such information is inferred by applying classical structural correlation criteria combined with microstructural analysis to test the compatibility of mineral assemblages that mark the successive foliations of different rock types (Delleani, Spalla, Castelli, & Gosso, 2013; Gosso et al., 2015; Hobbs, Means, & Williams, 1976; Passchier & Trouw, 2005; Roda & Zucali, 2011; Spalla, Siletto, di Paola, & Gosso, 2000; Spalla, Zucali, di Paola, & Gosso, 2005; Turner & Weiss, 1963; Williams, 1985; Zucali et al., 2002). On the map, outcropping rocks separated by drift cover have been represented with dark colours, whereas light colours have been used to draw the structural interpretation and show the complete outline of superposed structures. Dotted and full lines are used to convey interpretation confidence as constrained by the surface exposures. The Southern Sesia-Lanzo geological map employs the Technical Regional Topography of Piemonte Regional Administration (http://www.regione.piemonte.it), and the projection coordinate system is UTM ED50. The orientations of lithological boundaries, axial plane foliations, axial surfaces, fold axes and fractures are represented by equal-area Schmidt diagrams grouped according to their relative chronology and lithologic complexes. The most representative meso- and microstructural characteristics of the superposed fabric elements in the different lithotypes are shown in Figures 2–5. Two cross-sections at high angles to the fold axis of the D3 fold system highlight the 3D architecture of the tectonic contacts.

This type of map enables the visualisation of a complex structural framework together with its direct association, based on the related mineral assemblages, with the thermal regimes accompanying the development of superposed groups of structures. The map also facilitates the visualisation of rock volumes recording coherent sequences of tectono-metamorphic imprints, that is, coherent tectono-metamorphic histories (e.g. Salvi, Spalla, Zucali, & Gosso, 2010; Spalla, Gosso, Marotta, Zucali, & Salvi, 2010), and allows the immediate perception of their shared structural and metamorphic evolution.

4. Field data

4.1. Rock types

In the study area the RCT contains both crust- and mantle-derived rocks, the EMC mainly comprises protoliths of crustal continental origin, and the LM is composed of mantle-derived rocks. Mylonitic to ultramylonitic fabrics are widespread and are mainly concentrated at the contacts between the three complexes. These boundaries are characterised by a thick belt that has been marked on the map as an additional complex: the Mylonitic Zone (MZ) (Main Map), where the grain-size reduction makes the distinction of the protoliths difficult without the use of the microscope. In the following, a synthetic description of the rock types from the different complexes is provided and detailed descriptions of the superposed linear and planar fabrics and mineral assemblages are summarised in Table 1 while Figures 2–5 report macroscopic and microscopic photographs.

In the RCT, *gneisses* and *micaschists* are widespread and are characterised by alternating layers of quartz ± plagioclase ± epidote and blue–green amphibole + white mica and chlorite (Figure 2(a) and (b)). Locally, quartz-rich layers alternate with jadeite + white mica ± garnet layers (Figure 2(c)). Similarly, *orthogneisses* (Figure 2(d)) are characterised by fine-grained blue amphibole + white mica and quartz + K-feldspar layers alternating with mm to cm scales and marking the S2 foliation (Figure 2(e)). *Serpentinites* are generally thinly foliated and locally contain metre to decametre pods or lenses preserving pyroxenes (Figure 2(f) and (g)); relics of clinopyroxene and spinel also occur in types with mylonitic texture (Figure 2(h)). *Glaucophanites* are characterised by generally tectonitic to mylonitic texture (Figure 3(a)), in which S2 is marked by mm- to cm-thick alternating glaucophane + white mica- and quartz + epidote-rich layers (Figure 3(b)). *Metagabbros* occur as pods (Figure 3(c)) within glaucophanite and serpentinite and are characterised by granoblastic coronitic to tectonitic fabrics and locally occurring meter-thick layers of pyroxenite (Figure 3(d)). Clinopyroxene porfiroclasts are preserved, whereas plagioclase microsites are totally replaced by a fine-grained aggregate of white mica and epidote (Figure 3(e)).

In the EMC, *gneisses* and *micaschists* are the most common lithotypes (Figure 3(f)). The dominant foliation S2 is defined by the shape preferred orientation (SPO) of white mica + quartz ± epidote ± glaucophane (Figure 3(g) and (h)). Where S3 is pervasive, chlorite and white mica mark the foliation (Figure 3(g)), wrapping around porphyroclasts of chloritoid, glaucophane and garnet; jadeite is only locally preserved. *Glaucophanites* (Figure 4(a)) are banded rocks with alternating layers of glaucophane + white mica and quartz + epidote (Figure 4(b)). Locally, lawsonite porphyroclasts may occur, and greenschist retrogression is documented by the occurrence of actinolitic-amphibole and chlorite.

In the LM, *serpentinite* (Figure 4(c)) contains thin pyroxene-rich alternating with serpentine-rich layers: here the serpentine-bearing foliation wraps around clinopyroxene and opaque mineral porphyroclasts (Figure 4(d)).

The MZ includes all lithological types that have been observed in the three complexes in addition to silicate-bearing marbles. *Gneisses* and *micaschists* (Figure 4(e)) are composed of white mica + quartz + epidote ± plagioclase ± chlorite ± actinolite ± glaucophane and ± garnet (Figure 4(f)). The main fabric is defined by alternating quartz-rich layers and glaucophane + white mica-rich layers with a strong mylonitic to ultramylonitic S2 foliation. Locally a fine-grained foliation is marked by the SPO of white mica + chlorite and alternating actinolite-rich levels. *Orthogneisses* are composed of fine-grained jadeite, white mica, quartz, K-feldspar and garnet ± epidote (Figure 4(g) and (h)). Mylonitic to ultramylonitic fabric, frequently consisting of a compositional layering, is typically defined by rootless folds and S–C type foliations marked by jadeite trails and white mica + garnet-rich layers. K-feldspar porphyroclasts are wrapped by the mylonitic foliation and display tails of garnet and jadeite (Figure 4(g) and (h)). In the *silicates-bearing marbles* (Figure 5(a)), mm- to cm-thick carbonate-rich layers alternate with chloritoid + white mica layers, and pseudomorphosed lawsonite porphyroblasts occur locally (Figure 4(b)). Marbles occur as metre- to decametre-sized boudins within the mylonitic–ultramylonitic foliation. *Glaucophanites* (Figure 5(c)) contain glaucophane, white mica, ±epidote, ±quartz, ±garnet (Figure 5(d)). S2 mylonitic to ultramylonitic foliation is characterised by the SPO of glaucophane and white mica alternating with whitish quartz + epidote-rich layers. Lawsonite porphyroclasts are wrapped by the mylonitic foliation.

4.2. Structure and metamorphism

In the following section, meso- and microstructural features are described separately for the RCT, the

Table 1. Mineral associations and dominant textures in the different lithotypes of the EMC, RCT, LM and MZ. Mineral assemblages marking fabrics related to successive deformation stages (D1, D2, etc) are also specified, highlighting the differences of metamorphic environments in which successive fabrics developed in the different units.

	Rock type	Mineral mode	D1 fabric	D2 fabric	D3 fabric	D4 fabric
ROCCA Canavese Thrust Sheets	Gneiss and micaschist with alternate layers of Qtz ± Pl ± Ep and Amp + Wm and Chl. Locally Qtz-rich alternate layers with Jd + Wm bearing layers	Qtz ≤ 50%, Wm 5–40%, Amp (Gln/Act) 0–25%, Chl 5–25%, Jd 0–10%, Ep 0–35%, Pl 0–35%, Grt 0–10%	S1 foliation is generally marked by SPO of Gln, Wm, Qtz and rarely by Grt, Ep and opaque minerals. Locally a S1 mylonitic foliation is marked by alternating Jd + Wm ± Ep ± Grt and Qtz-rich layers, wrapping Grt, Jd and Ep porphyroblasts (Loc. Pendun)	S2 is defined by Qtz + Wm and Gln + Qtz compositional layering	S3 axial plane foliation of isoclinal folds is marked by SPO of Act + Chl + Wm	Mm- to cm- scale crenulation of S3 foliation locally associated with a differentiated rough foliation marked by fine-grained Chl and Wm
	Ortogneiss with layers of fine-grained Amp + Wm alternating with Qtz-Kfs rich layers at mm- to cm-scale	Qtz 20–35%, Kfs 5–20%, Wm 20–50%, Act 0–10%, Ep 0–15%, Gln 0–20%, opaque minerals 0–10%		S2 mylonitic foliation marked by mm-thick Gln + Wm + Ep and Kfs + Qtz compositional layering	S3 mylonitic foliation developed at low angle with S2 and marked by SPO and LPO of Act + Wm ± Qtz	
	Serpentinite: widely serpentinised granoblastic peridotite with relics of Cpx and Sp locally preserved in foliated types with mylonitic texture	Srp 90–100%, opaque minerals 0–5%, Cpx 0–5%		Generally mylonitic S2 foliation is marked by SPO of serpentine and opaque mineral trails	D3 crenulation with a 10 cm wavelength, locally associated with a differentiated S3 crenulation cleavage. S3 is marked by SPO of serpentine	
	Glaucophanite with mm- to cm-thick alternating layers of Gln + Wm and Qtz + Ep	Gln 10–40%, Wm 15–45%, Ep 0–10%, Qtz 0–10%, Act 0–10%, Chl 0–10%		S2 marked by mm-thick Gln + Wm and Ep + Qtz compositional layering	S3 foliation is marked by compositional layering between Act + Chl + Wm and Ep + Qtz layers. Locally D3 rootless isoclinal folds occur	
	Metagabbro generally with coronitic or tectonitic fabric. Where the texture is granoblastic Cpx porfiroclasts are preserved. Microdomains occupied by Ep + Wm represents replaced Pl. Cpx is partially replaced by Gl and CpxII. Metre-thick layers of pyroxenite locally occur	Di 30–50%, Chl 0–30%, Act 0–30%, Gln 0–20%, Wm 0–20%, Ep 0–15%, Pmp 0–15%, Grt 0–15%, Omph 0–10%		Discontinuous S2 foliation marked by SPO of Gln + Wm + Ep and Grt trails		
Eclogitic Micaschist Complex	Gneiss and micaschist with the dominant foliation defined by Wm + Chl + Qtz ± Ep with porphyroclasts of Cld or Gln and Grt. Locally Jd relics are preserved	Wm 5–40%, Qtz 0–50%, Pl 0–35%, Ep 0–35%, Chl 0–25%, Amp (Gln/Act) 0–25%, Grt 0–10%, Cld 0–10%, Jd 0–5%		S2 marked by Gln + Wm ± Ep ± Cld and Qtz-rich alternating layers	S3 axial plane foliation of isoclinal folds, from low angle to parallel to S2. S3 is marked by SPO of Act + Chl + Wm. S–C structures are diffused	
	Glaucophanite with mm-thick layers rich of Gln + Wm and rich of Qtz + Ep	Gln 10–50%, Wm 15–45%, Ep 0–10%, Qtz 0–10%, Act 0–10%, Grt 0–10%, Pl 0–10%, Chl 0–10%, Lws 0–5% (replaced by Wm, Zo/Czo ± Ab ± Chl)		S2 marked by mm-thick Gln + Wm and Ep + Qtz ± Lws pseudomorphs compositional layering. Gln and Wm show SPO	S3 axial planar foliation to isoclinal folds, from low angle to parallel to S2. S3 is marked by Act + Wm ± Chl-bearing thin layers. Pl-bearing veins crosscut S2.	

(*Continued*)

Table 1. Continued.

	Rock type	Mineral mode	D1 fabric	D2 fabric	D3 fabric	D4 fabric
Lanzo Massif	Serpentinite with alternating Cpx- and serpentine-bearing mineral layers, wrapping Cpxl and opaque mineral porphyroclasts	Srp 70–85%,Cpx 15–30%, opaque minerals 0–5%	S1 marked by SPO of serpentine and by equigranular aggregates of Cpxll	S2 crenulation cleavage, marked by SPO of serpentine, with 10 cm spacing		
Mylonitic Contact	Gneiss and micaschist with alternate layers of Qtz + Wm + Chl ± Pl ± Ep and Amp	Wm 15–50%, Qtz 15–40%, Amp (Gln/Act) 0–20%, Chl 5–10%, Ep 0–10%, Pl 0–10%, Grt 0–10%		S2 foliation, generally ultramylonitic, marked by compositional layering of Gln + Wm and Qtz ± Ep layers	S3 crenulation cleavage, often ultramylonitic. S3 is marked by SPO of Act + Chl + Wm and Pl + Ep ± Qtz layers. S–C structures are also common	
	Ortogneiss with layers of fine-grained Jd + Wm alternating with Qtz-rich layers at mm- to cm-scale	Qtz 25–30%, Kfs 0–15%, Wm 15–20%, Jd 20–35%, Ep 0–5%, Grt 0–5%	S1 foliation is better visible at the micro-scale and is marked by compositional layering between Jd + Wm ± Ep ± Grt, Qtz-rich and Wm-rich layer (Loc. Fandaglia). The S1 foliation wraps crystals of Grt, Jd, Kfs and Ep			
	Silicates-bearing marble with mm- to cm-thick Cal-rich alternate with Cld + Wm layers	Cal 40–70%, Cld ≤ 10%, Qtz ≤10%, Wm 10–20%, Lws ≤ 10%,Chl ≤10%, Grt < 5%, opaque minerals 5%.	Pre-S3 foliation is marked by Cld + Wm-bearing layers alternating with Cal-rich layers. Cld –Wm trails mark the internal foliation in Lws porphyroblasts		S3 crenulation cleavage is marked by SPO of Wm+ Chl + opaque minerals ± fine-grained quartz in thin layers	
	Glaucophanite with mm- to cm-thick layering of Gln + Wm and Qtz + Ep layers	Gln 10–50%, Wm 5–45%, Ep 0–30%, Qtz 0–15%, Act 0–20%, Pl 0–15%, Chl 0–10%, Grt 0–10%, Lws 0–5%, Pmp 0–5%	Better detectable at the micro-scale where the S1 foliation is marked by SPO of Gln, Wm, Qtz and rarely by Grt and Ep	S2 foliation, generally ultramylonitic, marked by compositional layering of mm-thick Gln + Wm and Ep + Qtz layers. Lws crystals are present as porphyroclasts, with inclusions of Gln, wrapped by S2 foliation or as inclusions in Grt	S3 axial planar foliation to isoclinal folds, commonly at low angle to parallel to S2. S3 is marked by Act + Chl + Wm and Pl + Ep ± Qtz layers. S–C structures are also common. Pmp + Chl aggregates replace Lws crystals	

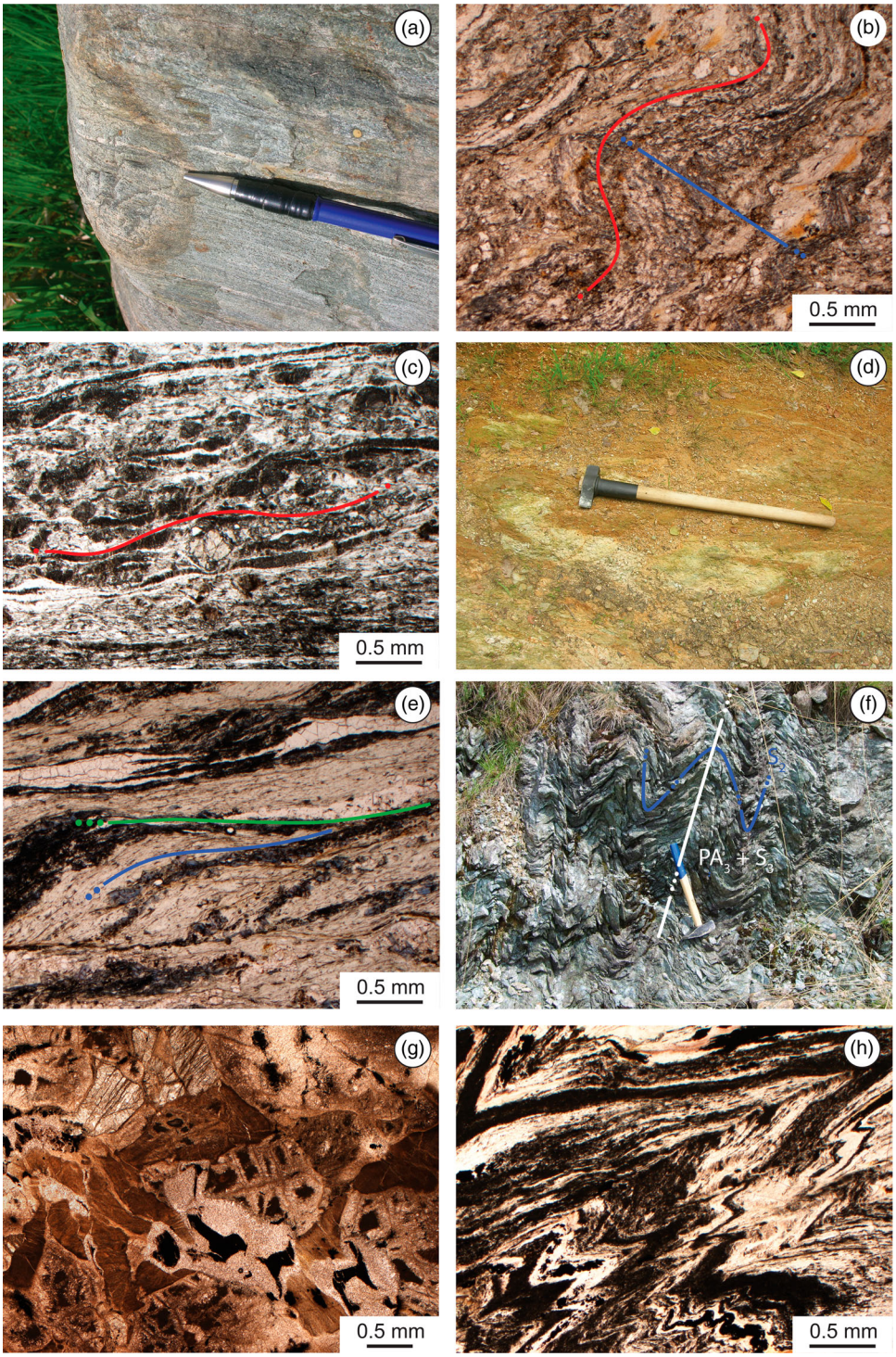

Figure 2. (a) Mineral layering marked by glaucophane-rich alternating with epidote-rich bands underlying S2 mylonitic foliation in gneiss of RCT (Rocca Canavese); (b) S1 foliation marked by glaucophane + white mica + quartz is bent during D2. A differentiated S2 axial plane foliation is underlined by SPO of glaucophane in gneiss from RCT (south of Truc Ariund) (plane polarised light); (c) S1 foliation marked by quartz-rich alternating with jadeite + white mica layers wraps syn-kinematic garnet porphyroclasts in gneisses from RCT (south of Rio Pendun) (plane polarised light); (d) sheets of serpentinites (green) in orthogneiss (brown) in RCT (east of Truc Ariund); (e) S2 and S3, marked by glaucophane + white mica + opaque minerals and chlorite + white mica respectively in orthogneiss from RCT (plane polarised light); (f) S2 marked by serpentine SPO folded during D3 in serpentinites from RCT (Madonna della Neve); (g) relict granoblastic texture in serpentinite from RCT: widely replaced by fine-grained serpentine, chlorite and opaque minerals (plane polarised light); (h) S2 marked by serpentine and opaque minerals alternating layers is bent by D3 microfolds in serpentinites from RCT (north of Madonna della Neve) (plane polarised light).

Eclogitic Micaschist Complex, the LM and the MZ. Table 1 schematically reports the distribution of the main structural features developed during successive deformation stages in all lithotypes, together with the mineral assemblages marking successive fabrics.

Figure 3. (a) S2 foliation marked by fine-grained glaucophane alternating with mm-thick quartz + epidote-rich layers and folded during D3 from a metre-thick layer of glaucophanites in gneisses of RCT (north of Rocca Canavese). A differentiated S3 axial plane foliation is marked by green amphibole. (b) S2 mylonitic foliation developed under blueschist facies conditions and marked by glaucophane, epidote, white mica and opaque minerals in epidote-rich glaucophanites from RCT (B. dei Signori) (crossed polars); (c) metagabbros of RCT (Madonna della Neve) locally with tectonitic fabric with S2 marked by glaucophane SPO; (d) large grains of clinopyroxene in granoblastic pyroxenite from RCT (crossed polars); (e) pumpellyite + tremolite + epidote + white mica aggregates replacing the plagioclase microsite in coronitic metagabbros from RCT (Madonna della Neve) (crossed polars); (f) D3 folding of S2 foliation marked by white mica + glaucophane. A differentiated S3 axial plane foliation is underlined by white mica in micaschists from EMC (T. Malone); (g) S2 foliation marked by glaucophane-rich alternating with quartz-rich layers is bent during D3 in gneisses from EMC (T. Malone). S3 axial plane foliation is marked by SPO of green amphibole (plane polarised light); (h) D3 fold of S2 foliation marked by white mica SPO micaschists from EMC (T. Malone) (crossed polars).

4.2.1. RCT

D1 – D1 is primarily observed as the S1 foliation at the micro-scale but is locally visible at the macro-scale (e.g. Rio di Pendun). The S1 foliation is preserved in micaschist and gneiss (Figure 2(b)) where it is marked by the SPO of white mica, amphibole and quartz. Rarely,

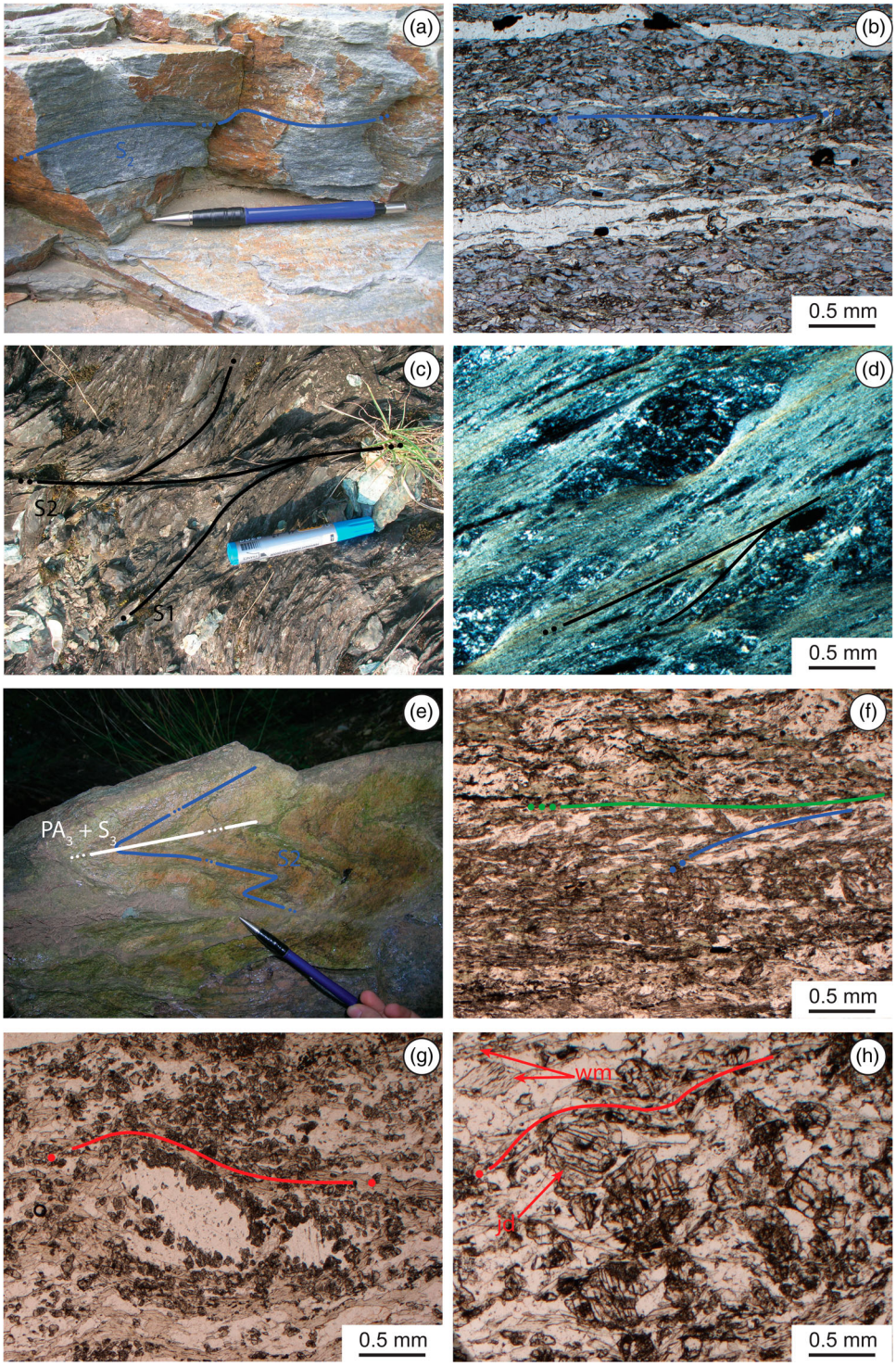

Figure 4. (a) S2 mylonitic foliation marked by glaucophane and white mica SPO in glaucophanites from EMC (T. Malone); (b) S2 mylonitic foliation marked by compositional layering of quartz-rich and glaucophane-rich layers in glaucophanites from EMC (T. Malone). Glaucophane shows SPO (plane polarised light); (c) S2 spaced foliation overprinting S1 in serpentinites of LM (T. Fandaglia); (d) mylonitic foliation with S–C planes wrapping opaque porphyroclasts in serpentinites from LM (T. Fandaglia) (crossed polars); (e) D3 folding of S2 foliation marked by SPO of glaucophane, white mica and epidote in gneisses of MZ (east of Case Fremt). A new axial plane foliation S3, which is marked by chlorite, white mica and opaque minerals, differentiates; (f) S3 mylonitic foliation marked by chlorite + white mica + green amphibole in gneisses from MZ (T. Fandaglia). Relics of S2 foliation, marked by glaucophane, is still preserved (plane polarised light); (g) S1 foliation marked by jadeite + white mica wrapping k-feldspar porphyroclasts in orthogneisses from MZ (T. Fandaglia). K-feldspar porphyroclasts show a rim of pseudomorphic jadeite; (h) S1 foliation is marked by jadeite and white mica and wraps jadeite porphyroclasts in aplitic veins in glaucophanites from MZ (west of Rocca Canavese).

epidote and garnet may occur as porphyroclasts, wrapped in the S1 foliation, whereas in pyroxenites granoblastic aggregates of clinopyroxene are well preserved (Figure 3(d)). S1 locally is characterised by a mylonitic fabric, defined by fine-grained jadeite, white mica, epidote and quartz-rich layers

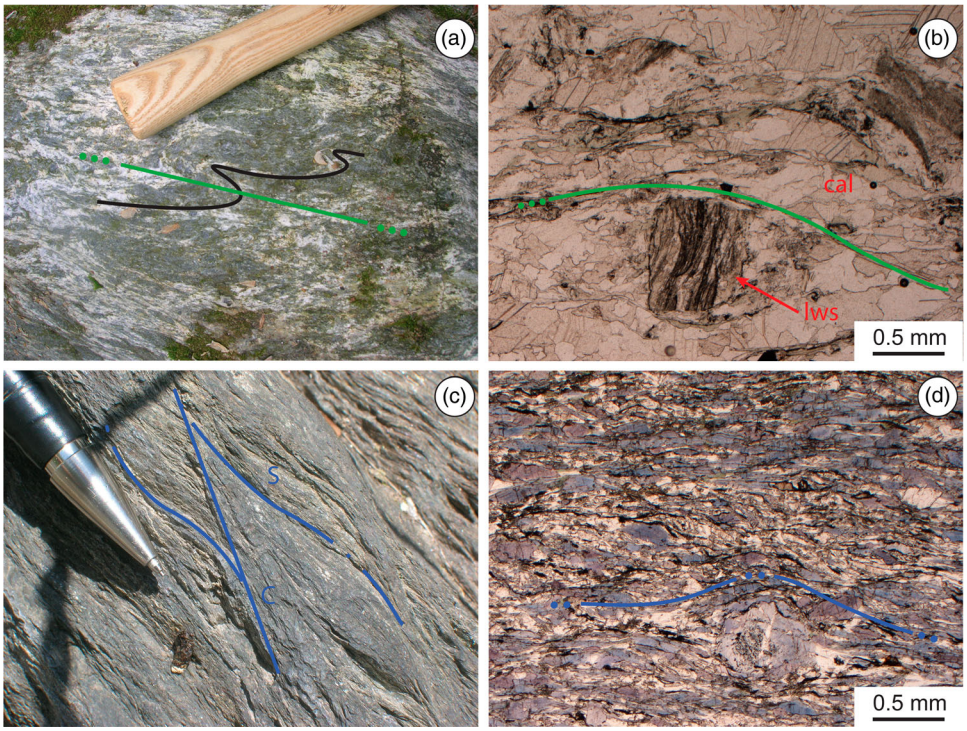

Figure 5. (a) Pre-S3 foliation (black) marked by compositional layering between chloritoid-rich and carbonate-rich layers is bent during D3 in silicate-bearing marble from MZ (T. Fandaglia). A differentiated S3 axial plane foliation is marked by chlorite + white mica; (b) S3 foliation, marked by chlorite, white mica and opaque minerals, wraps lawsonite porphyroclasts in silicate-bearing marble of MZ (T. Fandaglia) (plane polarised light); (c) Syn-D2 mylonitic fabric characterised by s–c planes marked by glaucophane and white mica in glaucophanites of MZ (T. Malone); (d) S2 foliation marked by glaucophane + white mica wraps syn-kinematic glaucophane porphyroclasts in glaucophanites from MZ (T. Fandaglia) (plane polarised light).

wrapping garnet, jadeite and epidote porphyroclasts (Figure 2(c)).

D2 – The S2 fabric is the most pervasive in all lithotypes. D2 is also related to the development of mylonitic to ultramylonitic foliations in orthogneiss (Figure 2(e)). Compositional layering and the SPO of glaucophane, white mica, quartz and epidote define the S2 foliation in the gneisses, orthogneiss and micaschists (Figure 2(b) and (e)). In glaucophanite, S2 is marked by the SPO of glaucophane and white mica alternating with epidote, quartz and plagioclase-rich layers and locally is mylonitic (Figure 3(b)); in metagabbro, S2 is defined by garnet trails, glaucophane and white mica-rich layers. In serpentinite, S2 is marked by serpentine SPO and opaque mineral trails (Figure 2(h)).

D3 – D3-related structures consist of a centimetre to metre-scale folding, associated with the development of an S3 axial plane foliation (Figure 3(a)). The S3 foliation may have mylonitic features and is commonly defined by a mineral compositional layering marked by the SPO of white mica, green amphibole, chlorite, epidote and quartz in crustal rocks (Figure 2(c) and (e)). In serpentinite S3 is defined by the SPO of serpentine (Figure 2(h)). Locally coronitic minerals overgrew clinopyroxene porphyroclasts in metagabbros (Figure 3(e)) and granoblastic aggregates in serpentinites (Figure 2(g)).

D4 – D4 consists of a centimetre-scale crenulation, locally associated with a rough cleavage, and marked by chlorite and white mica SPO.

Poles to foliation planes S1 + S2 and S3, shown on the map, display heterogeneous distributions. Specifically, they describe a main cluster oriented W–NW dipping between 45 and 70 degrees within a broad girdle dipping W–SW at approximately 30 degrees. Such a dispersed distribution of foliations cannot be easily related to large-scale folding, although an axial plane, broadly striking at NW–SE, can be recognised. The few orientation data acquired for D4 axial planes and axes within the RCT prevent any confident correlation, even if their distribution is compatible with the dispersion of earlier fabric elements. Post-D4 steeply dipping fractures are widespread and commonly dip NE, SE and SW.

4.2.2. EMC

D1 – In the limited portion of the EMC mapped here, no relict D1 structures have been found to correspond with the geometric characteristics and orientations of those occurring in the surrounding areas (Spalla & Zulbati, 2003). In these areas S1 is exclusively observed in eclogite boudins, which is contemporaneous with the development of the assemblage omphacite + epidote + rutile ± amphibole ± garnet + quartz.

D2 – The Eclogitic Micaschist Complex is characterised by a penetrative foliation (S2) marked by blueschist facies assemblages in gneiss (Figure 3(g) and (h)) and glaucophanite (Figure 4(b) and Table 1). The glaucophane and white mica SPOs mark the S2

foliation along mm- to cm-thick layers alternating with quartz ± epidote ± plagioclase-rich layers (Figure 3(h)).

D3 – The D3 deformation produces metre- to ten of meters-scale folds associated with the pervasive development of an S3 axial plane foliation and the growth of greenschist facies assemblages that mark the new fabrics. S3 is defined by the SPO of actinolitic-amphibole + chlorite + white mica (Figure 3(g) and (h)). Mylonitic S–C structures are widespread in glaucophanite and gneiss.

The orientations of poles to the S1 + S2 planes display a weak girdle distribution that agrees with the NW–SE strike of an axial plane, associated with a steeply dipping axis toward the SE. S3 poles to the foliation plot close to the orientation of the above-inferred axial plane. No D4 structures have been observed in the field, whereas post-D4 fractures show various and dispersed orientations.

4.2.3. LM

D1 – The LM occupies a small area of the map and is characterised by a mylonitic foliation (S1) defined by the SPO of serpentine fibres (Figure 4(d)) and equigranular aggregates of clinopyroxene.

D2 – Locally, a D2 crenulation is present and a new S2 axial plane foliation is developed. The S2 is a crenulation cleavage, marked by the SPO of serpentine, with 10-cm spacing.

4.2.4. MZ

D1 – D1 in the MZ is defined by a micro-scale S1 foliation recorded in orthogneiss (Figure 4(g)) and glaucophanite (Figure 4(h)). S1 is defined by compositional layering and the SPOs of white mica, quartz, epidote and jadeite in gneiss and micaschist, and by alternating glaucophane- and epidote-rich layers in glaucophanite. In silicate-bearing marbles a pre-S3 foliation is recorded, commonly defined by chloritoid and white mica layers alternating with carbonate-rich layers, locally preserved within lawsonite porphyroblasts (Figure 5(b)).

D2 – The S2 foliation is the most common feature in the MZ. It is defined by a mylonitic to ultramylonitic foliation marked by compositional layering and the SPO of glaucophane, white mica, epidote and quartz (Figures 4(f) and 5(d)). Lawsonite porphyroclasts are locally wrapped by the S2 foliation in glaucophanite.

D3 – D3 consists of tight to isoclinal folds at various scales, from centimetres to tens of metres in the MZ between the RCT and the EMC. D3 folds are associated with the development of S3 crenulation cleavage or disjunctive foliation. S3 commonly has a low angle with respect to S2 and is marked by the SPOs of green amphibole, white mica, chlorite, plagioclase, epidote and quartz (Figure 4(f)). S–C mylonitic structures may also occur in glaucophanite and gneiss. Pumpellyite and chlorite aggregates define pseudomorphs after lawsonite crystals. D3 in the MZ between the LM and the RCT is responsible for the development of a composite ultramylonite fabric S2/S3 in glaucophanites along Torrente Fandaglia, resulting from the granular-scale reactivation of S2 during D3. Here, no D3 folds have been observed.

D4 – Locally, a decimetre- to centimetre-scale crenulation can be detected, in places associated with a differentiated cleavage defined by chlorite and white mica SPOs and dipping 45–50° eastward.

Within the MZ, the distribution of S1 + S2 and S3 poles to the foliations is much less variable (Main Map). Both groups of data display a strong clustering around SW and a dip angle between 0 and 25°. This distribution is easily related to the mylonitic to ultramylonitic character of these structures. Steeply dipping D3 axial planes also strike NW–SE and are associated with steeply to moderately dipping axes. Post-D4 fractures are less widespread than in the RCT and commonly dip steeply with variable dip directions.

5. Summary and conclusions

The multiscale structural analysis performed to produce this map of the southern SLZ indicates that the sequence of Alpine deformation stages is different in EMC, RCT, MZ and LM rocks. Four synmetamorphic fabrics have been detected in the RCT and MZ, whereas D4 folds and foliations are lacking in the EMC and LM, thus indicating the low pervasiveness of these late structures. D1 and D2 are responsible for the lenticularisation and transposition of lithostratigraphy, as demonstrated by the hectometre-scale gabbro boudins in the serpentinite and glaucophanite and by the glaucophanite lenses in the gneiss and micaschist. In the four mapped complexes (RCT, EMC, LM and MZ), S2 is the dominant foliation in all rock types and is generally mylonitic, evolving up to ultramylonitic in the MZ. In contrast, S1 is observed only locally at the meso-scale in the RCT and LM and detected exclusively at the micro-scale in the MZ. In the EMC, S1 relicts are described NNW of the mapped region (Spalla & Zulbati, 2003) in eclogite boudins, in which S1 is defined by the SPO of omphacite. Similar pre-metamorphic textures and mineral relics have been detected exclusively at Madonna della Neve in gabbro boudins. The rare exposed lithologic boundaries are parallelised to the dominant foliation (S2). S2 is subvertical, as are the lithotectonic slices belonging to the different metamorphic complexes, which show a tectonic setting similar to that of the Southern Steep Belt (Schmid et al., 1996) that rims the Periadriatic Lineament in Central Alps. Additionally, foliations (insets A and B and Schmidt nets on the map) lie at a low angle or parallel to the Periadriatic Lineament, that is named the Canavese Line in this portion of the Alpine chain. The MZ between the LM and the

RCT is straight and trends NW–SE, whereas between the EMC and the RCT, it is deformed by tight to isoclinal D3 folds, locally associated with the development of a generally N–S trending axial plane S3 foliation. The ultramylonitic nature of structures at Torrente Fandaglia within MZ suggest the interpretation represented on the Map and cross-section, where the contact is represented as a km-scale shear zone that was active from blueschist (D2) to greenschist (D3) conditions, associated with the occurrence of kilometre-scale asymmetric folding.

The association of relative fabric age and metamorphic environment is not univocal across the mapped area. D1 deformation developed under eclogite-facies conditions in the EMC and under blueschist facies conditions in the RCT. Blueschist mineral assemblages marking D2 fabrics in the EMC are equivalent to those marking D2 fabrics in the RCT; the same equivalence exists between syn-D3 mineral assemblages in the EMC and the RCT, both under greenschist facies conditions. Serpentinite in the LM unfortunately contains mineral assemblages that are 'insensitive' to the transitions from eclogite to blueschist facies conditions. However, the occurrence of mineral assemblages accounting for PT values at the boundary with ultra-high pressure conditions (Viù Valley; Pelletier & Muentener, 2006) in metagabbro dykes from the southwestern prolongation of the LM indicates that eclogite-facies conditions predated the development of the D2 structures here as well. Differences in metamorphic evolutions between the EMC, LM and RCT shown by the PT trajectories reported in Figure 1 have, as already noted, been known for a long time, but the multiscale structural analysis synthesised in this new map allows the correlation between superposed fabrics and metamorphic imprints across the different units. Foliation trajectories on the map, representing the finite strain field by means of the configuration of planar fabrics, and containing systematic information on mineral assemblages associated with successive foliations, allow us to infer that the mylonitic to ultramylonitic S2 foliation characterising the tectonic boundary (MZ) between the EMC, the RCT, and the LM developed under blueschist facies conditions. Because the eclogite facies metamorphic imprint and the related fabric is recorded exclusively in EMC and LM rocks, these units experienced a deeper tectonic trajectory than the RCT rocks, which ubiquitously record their climax conditions under blueschist facies. The coupling between the EMC, RCT and LM occurred during the blueschist facies re-equilibration recorded in the course of exhumation-related decompression. The occurrence of greenschist mylonites, which commonly rework the earlier blueschist mylonitic bands, indicates that the tectonic contact was reactivated at shallower crustal levels during the final stages of uplift. The chosen mapping technique, highlighting relationships between metamorphic assemblages and superposed fabrics, demonstrates that blueschist facies was the environment under which the three metamorphic complexes coupled into a unique tectono-metamorphic unit, sharing D2 and the successive structural and metamorphic re-equilibration stages during their exhumation by the subduction system.

Software

The graphical design of the map was produced using Adobe Illustrator CS6 from points, polylines and polygons exported from a GIS. Equal-area Schmidt diagrams were produced using Stereonet (Allmendinger, 2002–2015).

Acknowledgements

Funding is acknowledged from PRIN 2010–2011 'Birth and death of oceanic basins: geodynamic processes from rifting to continental collision in Mediterranean and Circum-Mediterranean orogens'. C. Malinverno provided the thin sections. Fieldwork was performed by M.C. and L.S. during their Master and Bachelor work, respectively. Microstructural analysis was the subject of M.C.'s Master work. M.Z. and M.I.S. supervised the fieldwork. American Journal Expert reviewed the English grammar and syntax.

Disclosure statement

No potential conflict of interest was reported by the authors.

Funding

This work was supported by the PRIN 2010–2011: 'Birth and death of oceanic basins: geodynamic processes from rifting to continental collision in Mediterranean and Circum-Mediterranean orogens'.

References

Allmendinger, R. W. (2002–2015). Retrieved from http://www.geo.cornell.edu/geology/faculty/RWA/programs/stereonet.html

Avigad, D. (1996). Precollisional ductile extension in the internal western Alps (Sesia zone). *Earth and Planetary Science Letters*, *137*, 175–188.

Babist, J., Handy, M. R., Konrad-Scmolke, M., & Hammerschmidt, K. (2006). Precollisional, multistage exhumation of subducted continetal crust: The Sesia Zone, Western Alps. *Tectonics*, *25*, TC6008. doi:10.1029/2005TC001927

Barnes, J. D., Beltrando, M., Lee, C.-T. A., Cisneros, M., Loewy, S., & Chin, E. (2014). Geochemistry of Alpine serpentinites from rifting to subduction: A view across paleogeographic domains and metamorphic grade. *Chemical Geology*, *389*, 29–47.

Bertotti, G., Siletto, G. B., & Spalla, M. I. (1993). Deformation and metamorphism associated with crustal rifting: Permian to Liassic evolution of the Lake Lugano-Lake Como area (Southern Alps). *Tectonophysics*, *226*, 271–284.

Bertotti, G., & der Voorde, M. (1994). Thermal effects of normal faulting during rifted basin formation, 2. The Lugano-Valgrande normal fault and the role of pre-existing thermal anomalies. *Tectonophysics*, *240*, 145–157.

Boudier, F. (1978). Structure and petrology of the Lanzo peridotite massif (Piedmont Alps). *Geological Society of America Bulletin*, *89*, 1574–1591.

Cenki-Tok, B., Oliot, E., Rubatto, D., Berger, A., Engi, M., Janots, E., … Goncalves, P. (2011). Preservation of Permian allanite within an Alpine eclogite facies shear zone at Mt Mucrone, Italy: Mechanical and chemical behavior of allanite during mylonitization. *Lithos*, *125*, 40–50.

Compagnoni, R., Dal Piaz, G. V., Hunziker, J. C., Gosso, G., Lombardo, B., & Williams, P. F. (1977). The Sesia-Lanzo Zone: A slice of continental crust, with alpine HP-LT assemblages in the Western Italian Alps. *Rendiconti della Società Italiana di Mineralogia e Petrologia*, *33*, 281–334.

Dal Piaz, G. V. (1993). Evolution of Austroalpine and Upper Penninic basement in the Northwestern Alps from Variscan convergence to post-Variscan extension. In J. Von Raumer & F. Neubauer (Eds.), *Pre-Mesozoic geology in the Alps* (pp. 325–342). Berlin: Springer.

Dal Piaz, G. V., Gosso, G., & Martinotti, G. (1971). La II Zona Diorito-kinzigitica tra la Valsesia e la Valle d'Ayas (Alpi occidentali). *Memorie della Società Geologica Italiana*, *10*, 257–276.

Dal Piaz, G. V., Hunziker, J. C., & Martinotti, G. (1972). La Zona Sesia-Lanzo e l'evoluzione tettonico-metamorfica delle Alpi Nordoccidentali interne. *Memorie della Società Geologica Italiana*, *11*, 433–460.

Delleani, F., Spalla, M. I., Castelli, D., & Gosso, G. (2013). A new petrostructural map of Monte Mucrone metagranitoids (Sesia-Lanzo Zone, Western Alps). *Journal of Maps*, *9*, 410–424. doi:10.1080/17445647.2013.800004

Diella, V., Spalla, M. I., & Tunesi, A. (1992). Contrasted thermo-mechanical evolutions in the Southalpine metamorphic basement of the Orobic Alps (Central Alps, Italy). *Journal of Metamorphic Geology*, *10*, 203–219.

Gosso, G. (1977). Metamorphic evolution and fold history in the eclogite micaschists of the upper Gressoney valley (Sesia-Lanzo zone, Western Alps). *Rendiconti della Società Italiana di Mineralogia e Petrologia*, *33*, 389–407.

Gosso, G., Rebay, G., Roda, M., Spalla, M. I., Tarallo, M., Zanoni, D., & Zucali, M. (2015). Taking advantage of petrostructural heterogeneities in subduction-collisional orogens, and effects on the scale of analysis. *Periodico di Mineralogia*, *84*(*3B*), 779–825.

Handy, M. R., Franz, L., Heller, F., Janott, B., & Zurbriggen, R. (1999). Multistage accretion and exhumation of the continental crust (Ivrea crustal section, Italy and Switzerland). *Tectonics*, *18*(*6*), 1154–1177.

Handy, M. R., & Oberhaensli, R. (2004). Explanatory notes to the map: Metamorphic structure of the Alps – Age map of metamorphic structure of the Alps – Tectonic interpretation and outstanding problems. *Mitteilungen der Österreichischen Mineralogischen Gesellschaft*, *149*, 201–225.

Hobbs, B. E., Means, W. D., & Williams, P. F. (1976). *An outline of structural geology*. New York, NY: Wiley.

Hunziker, J. C. (1974). Rb/Sr and K/Ar age determination and the Alpine tectonic history of the Western Alps. *Mem. Istituto di Geolologia e Mineralogia dell' Università di Padova*, *31*, 1–55.

Hunziker, J. C., Desmons, J., & Hurford, A. J. (1992). Thirty-two years of geochronological work in the Central and Western Alps: A review on seven maps. *Mémoires de Géologie Lausanne*, *13*, 1–59.

Kienast, J. R., & Pognante, U. (1988). Chloritoid-bearing assemblages in eclogitized metagabbros of the Lanzo peridotite body (western Italian Alps). *Lithos*, *21*, 1–11.

Lardeaux, J. M. (1981). *Evolution tectono-metamorphique de la zone nord du Massif de Sesia-Lanzo (Alpes occidentales): un exemple d'éclogitisation de croute continentale* (PhD Thesys), Université Paris VI, 226 pp.

Lardeaux, J. M., & Spalla, M. I. (1991). From granulites to eclogites in the Sesia zone (Italian Western Alps): A record of the opening and closure of the Piedmont Ocean. *Journal of Metamorphic Geolology*, *9*, 35–59.

Manzotti, P., & Zucali, M. (2013). The pre-Alpine tectonic history of the Austroalpine continental basement in the Valpelline unit (Western Italian Alps). *Geological Magazine*, *150*(*1*), 153–172. doi:10.1017/s0016756812000441

Marotta, A. M., Spalla, M. I., & Gosso, G. (2009). Upper and lower crustal evolution during lithospheric extension: Numerical modelling and natural footprints from the European Alps. *Geological Society of London Special Publications*, *321*, 33–72.

Nicolas, A. (1974). Mise en place des péridotites de Lanzo (Alpes piémontaises); relation avec tectonique et métamorphisme alpins; conséquences géodynamiques. *Schweizerische Mineralogische Petrographische Mitteilungen*, *54*, 449–460.

Oberhaensli, R., Hunziker, J. C., Martinotti, G., & Stern, W. B. (1985). Geochemistry, gheochronology and Petrology of Monte Mucrone: An example of Eo-Alpine eclogitisation of Permian granitoids in the Sesia-Lanzo Zone, Western Alps, Italy. *Chemical Geology*, *52*, 165–184.

Passchier, C. W., & Trouw, R. A. J. (2005). *Microtectonics*. Berlin: Springer.

Pelletier, L., & Muentener, O. (2006). High-pressure metamorphism of the Lanzo peridotite and its oceanic cover, and some consequences for the Sesia-Lanzo zone (northwestern Italian Alps). *Lithos*, *90*, 111–130.

Piccardo, G. B. (2010). The Lanzo peridotite massif, Italian Western Alps: Jurassic rifting of the Ligurian Tethys. *Geological Society of London Special Publications*, *337*, 47–69.

Piccardo, G. B., Zanetti, A., Pruzzo, A., & Padovano, M. (2007). The North Lanzo peridotite body (NW Italy): Lithospheric mantle percolated by MORB and alkaline melts. *Periodico di Mineralogia*, *76*(*2–3*), 199–221.

Pognante, U. (1989a). Lawsonite, blueschist and eclogite formation in the southern Sesia Zone (Western Alps, Italy). *European Journal of Mineralogy*, *1*, 89–104.

Pognante, U. (1989b). Tectonic implications of lawsonite formation in the Sesia zone (Western Alps). *Tectonophysics*, *162*, 219–227.

Pognante, U. (1991). Petrological constraints on the eclogite- and blueschist-facies metamorphism and P-T-t paths in the Western Alps. *Journal of Metamorphic Geology*, *9*, 5–17.

Pognante, U., Talarico, F., & Benna, P. (1987). Incomplete blueschist re-crystallization in high grade metamorphics from the Sesia-Lanzo unit (Vasario – Sparone subunit, Western Alps ophiolites): A case history of metastability. *Lithos*, *21*, 129–142.

Rebay, G., & Spalla, M. I. (2001). Emplacement at granulite facies conditions of the Sesia-Lanzo metagabbros: An early record of Permian rifting? *Lithos*, *58*, 85–104.

Regis, D., Rubatto, D., Darling, J., Cenki-Tok, B., Zucali, M., & Engi, M. (2014). Multiple metamorphic stages within an eclogite-facies terrane (Sesia Zone, Western Alps) revealed by Th-U-Pb petrochronology. *Journal of Petrology*, *55*, 1429–1456.

Roda, M., Marotta, A. M., & Spalla, M. I. (2010). Numerical simulations of an ocean-continent convergent system: Influence of subduction geometry and mantle wedge hydration on crustal recycling. *Geochemistry Geophysics Geosystems*, *11*, 1–21.

Roda, M., Spalla, M. I., & Marotta, A. M. (2012). Integration of natural data within a numerical model of ablative subduction: A possible interpretation for the Alpine dynamics of the Austroalpine crust. *Journal of Metamorphic Geology*, *30*, 973–996.

Roda, M., & Zucali, M. (2011). Tectono-metamorphic map of the Mont Morion Permian metaintrusives (Mont Morion-Mont Collon-Matterhorn Complex, Dent Blanche Unit), Valpelline-Western Italian Alps. *Journal of Maps*, *7*, 519–535. doi:10.4113/jom.2011.1194

Rubatto, D. (1998). *Dating of pre-Alpine magmatism, Jurassic ophiolites and Alpine subductions in the western Alps* (Unpublished PhD thesis). ETH, Zürich.

Rubatto, D., Gebauer, D., & Compagnoni, R. (1999). Dating of eclogit-facies zircons; the age of Alpine metamorphism in Sesia-Lanzo Zone (Western Alps). *Earth and Planetary Science Letters*, *167*, 141–158.

Rubatto, D., Regis, D., Hermann, J., Boston, K., Engi, M., Beltrando, M., & McAlpine, S. R. B. (2011). Yo-yo subduction recorded by accessory minerals in the Italian Western Alps. *Nature Geoscience*, *4*, 338–342.

Salvi, F., Spalla, M. I., Zucali, M., & Gosso, G. (2010). Three-dimensional evaluation of fabric evolution and metamorphic reaction progress in polycyclic and polymetamorphic terrains: A case from the Central Italian Alps. *Geological Society of London Special Publications*, *332*, 173–187.

Schmid, S. M., Berger, A., Davidson, C., Gieré, R., Hermann, J., Nievergelt, P., … Rosenberg, C. (1996). The Bergell Pluton (Southern Switzerland-Northern Italy): Overview accompanying a geological-tectonic map of the intrusion and surrounding country rocks. *Schweizerische Mineralogische Petrographische Mitteilungen*, *76*, 329–355.

Schuster, R., Scharbert, S., Abart, R., & Frank, W. (2001). Permo-Triassic extension and related HT/LP metamorphism in the Austroalpine-Southalpine realm. *Mitteilungen der Gesellschaft der Geologie und Bergbaustudenten in Oesterreich*, *45*, 111–141.

Schuster, R., & Stuewe, K. (2008). Permian metamorphic event in the Alps. *Geology*, *36*(*8*), 603–606.

Spalla, M. I., De Maria, L., Gosso, G., Miletto, M., & Pognante, U. (1983). Deformazione e metamorfismo della Zona Sesia – Lanzo meridionale al contatto con la falda piemontese e con il massiccio di Lanzo, Alpi occidentali. *Memorie della Società Geologica Italiana*, *26*, 499–514.

Spalla, M. I., Gosso, G., Marotta, A. M., Zucali, M., & Salvi, F. (2010). Analysis of natural tectonic systems coupled with numerical modelling of the polycyclic continental lithosphere of the Alps. *International Geology Review*, *52*, 1268–1302.

Spalla, M. I., Lardeaux, J. M., Dal Piaz, G. V., & Gosso, G. (1991). Metamorphisme et tectonique a la marge externe de la zone Sesia-Lanzo (Alpes occidentales). *Memorie della Società Geologica*, *43*, 361–369.

Spalla, M. I., Lardeaux, J. M., Dal Piaz, G. V., Gosso, G., & Messiga, B. (1996). Tectonic significance of alpine eclogites. *Journal of Geodynamics*, *21*, 257–285.

Spalla, M. I., Siletto, G. B., di Paola, S., & Gosso, G. (2000). The role of structural and metamorphic memory in the distinction of tectono-metamorphic units: The basement of the Como Lake in the Southern Alps. *Journal of Geodynamics*, *30*, 191–204.

Spalla, M. I., Zanoni, D., Marotta, A. M., Rebay, G., Roda, M., Zucali, M., & Gosso, G. (2014). The transition from Variscan collision to continental break-up in the Alps: Insights from the comparison between natural data and numerical model predictions. *Geological Society of London Special Publications*, *405*, 363–400. Retrieved from http://dx.doi.org/10.1144/SP1405.1111

Spalla, M. I., Zucali, M., di Paola, S., & Gosso, G. (2005). A critical assessment of the tectono-thermal memory of rocks and definition of tectono-metamorphic units: Evidence from fabric and degree of metamorphic transformations. *Geological Society of London Special Publications*, *243*, 227–247.

Spalla, M. I., & Zulbati, F. (2003). Structural and Petrographic map of the Southern Sesia-Lanzo Zone (Monte Soglio – Rocca Canavese, Western Alps, Italy). *Memorie di Scienze Geologiche, Padova*, *55*, 119–127.

Stoeckhert, B., Jaeger, E., & Voll, G. (1986). K-Ar age determinations on phengites from the internal part of the Sesia zone, lower Aosta Valley (Western Alps, Italy). *Contributions to Mineralogy and Petrology*, *92*, 456–470.

Stuenitz, H. (1989). *Partitioning of metamorphism and deformation in the boundary region of the "Seconda Zona Diorito-Kinzigitica", Sesia Zone, Western Alps* (Unpublished PhD thesis). ETH, Zurich.

Turner, F. J., & Weiss, L. E. (1963). *Structural analysis of metamorphic tectonites*. New York, NY: MacGraw-Hill.

Wheeler, J., & Butler, R. W. H. (1993). Evidence for extension in the western Alpine orogen: The contact between the oceanic Piemonte and overlying continental Sesia units. *Earth and Planetary Science Letters*, *117*, 457–474.

Williams, P. F. (1985). Multiply deformed terrains – Problems of correlation. *Journal of Structural Geology*, *7*, 269–280.

Williams, P. F., & Compagnoni, R. (1983). Deformation and metamorphism in the Bard area of the Sesia Lanzo Zone, Western Alps, during subduction and uplift. *Journal of Metamorphic Geology*, *1*, 117–140.

Wogelius, R. A., & Finley, F. C. (1989). Subsolidus emplacement history of the Lanzo Massif, Northern Italy. *Geology*, *17*, 995–998.

Zucali, M. (2011). Coronitic microstructures in patchy eclogitised continental crust: The Lago della Vecchia Permian metagranite (Sesia-Lanzo Zone, Western Italian Alps). *Journal of the Virtual Explorer*, *38*, paper 7, 1–28.

Zucali, M., & Spalla, M. I. (2011). Prograde lawsonite during the flow of continental crust in the Alpine subduction: Strain vs. metamorphism partitioning, a field-analysis approach to infer tectonometamorphic evolutions (Sesia-Lanzo Zone, Western Italian Alps). *Journal of Structural Geology*, *33*, 381–398.

Zucali, M., Spalla, M. I., & Gosso, G. (2002). Fabric evolution and reaction rate as correlation tool: The example of the Eclogitic Micaschists complex in the Sesia-Lanzo Zone (Monte Mucrone – Monte Mars, Western Alps Italy). *Schweizerische Mineralogische Petrographische Mitteilungen*, *82*, 429–454.